

# Net-Form Manufacturing of Aluminum Components: the Dependence of Processing Parameters on Component Quality

By Melissa Orme<sup>†</sup>, Qingbin Liu<sup>†</sup>, Robert Smith<sup>†</sup>, Charles Huang<sup>†</sup>, and John Fischer<sup>‡</sup>

<sup>†</sup>Department of Mechanical and Aerospace Engineering  
University of California, Irvine 92607-3975

<sup>‡</sup>Boeing Commercial Airplane Group, P.O. Box 3707, MC 5L-14  
Seattle, WA 98124-2207

## ABSTRACT

High precision droplet-based net-form manufacturing of structural components is gaining considerable academic and industrial interest due to the promise of improved component quality resulting from rapid solidification processing and the economic benefits associated with fabricating a structural component in one integrated operation. In this work circular cylinders that are 35 mm in diameter and up to 11 cm in height are fabricated in their net-form by depositing molten 2024 aluminum alloy droplets onto a flat-plate substrate and building the cylinder layer by layer in the direction of its long axis. Droplets are generated from capillary stream break-up from 150-micron diameter orifices at rates typically on the order of 18,000 droplets/second depending on stream conditions. The mechanical and microstructural characteristics of the net-formed components are studied and their dependence on the processing parameters such as droplet temperature, substrate temperature and mass flow rate delivered to the substrate is ascertained.

## Introduction

A droplet-based net-form manufacturing technique is under development at UCI which is termed Precision Droplet-Based Net-Form Manufacturing (PDM). The crux of the technique lies in the ability to generate highly uniform streams of molten metal droplets such as aluminum or aluminum alloys. Though virtually any metal that can be melted and contained in a crucible is suitable for use with PDM, the results presented in this paper focus on droplet deposition with molten aluminum alloy (2024) droplet streams that are generated from capillary stream break-up in an inert environment (Argon or Nitrogen). Other results that concentrate on fabrication of pure aluminum components with PDM are presented elsewhere.<sup>1</sup> In the final realization of the PDM process, the droplets will be electrostatically charged and deflected onto the substrate where they “splat,” which entails simultaneous spreading and solidification. The charging and deflection of droplets bears many similarities to the technology of ink-jet printing,<sup>2, 3</sup> except that in the current application of PDM, the droplet charges are significantly higher in order to print large lateral areas. We have found that large electrostatic charges on closely spaced droplets can result in mutual inter-droplet interactions,<sup>4</sup> which are not evident in the ink-jet printing technology. Successive droplet deliveries build a component layer by layer.

Figure 1 illustrates the generation of molten metal droplet streams from capillary stream break-up. The orifice diameter is 150 microns, which, for the conditions employed in this work, results in 284  $\mu\text{m}$  diameter droplets. The droplet stream speed,  $V$ , was varied over the range of 10 m/s to 13 m/s, and the droplet production frequency,  $f$ , was varied according to the relation

$f = (k_o^* V) / (2\pi r_o)$ , where  $k_o^*$  is the nondimensional wavenumber equal to the ratio of the stream circumference to the wavelength,  $\lambda$ , of the applied disturbance. It is well known in the field of droplet formation from capillary stream break-up that the fastest growing disturbance on an inviscid capillary stream occurs when  $k_o^*$  is equal to 0.697.<sup>5,6,7</sup> Most molten metals can be approximated as inviscid. It has also been

shown in previous work, that droplet generation at the  $k_o^*$  of the fastest growing disturbance results in the most uniform droplet stream.<sup>8</sup> Using the above relation for  $f$  insures equally spaced droplets at a variety of droplet speeds with droplet production frequencies in the range of 15,000 Hz to 19,000 Hz for the droplet speeds employed in this work.

PDM bears similarities with other emerging technologies of net-form manufacturing such as Shape Deposition Manufacturing, SDM,<sup>9,10,11,12</sup> and 3-D printing.<sup>13</sup> In SDM, a feedstock wire located directly over the substrate is melted using a plasma-welding torch. A discrete droplet of typical dimension 1-10 mm (depending on plasma conditions) falls off the wire and onto the substrate and builds the material component by droplet deposition at a rate on the order of 100 Hz, i.e., over two orders of magnitude slower than with the PDM technology. The advantage of SDM is that refractory metals can be melted with the plasma-welding torch.

In 3-D Printing, a green part is created by printing a stream of binder droplets onto a metal powder bed according to CAD information. However in that process, several post-treatment steps are necessary to insure a mechanically sound component.

As an intermediate step in the development of the PDM process, we have chosen to fabricate circular cylinders by depositing molten aluminum 2024 alloy droplets onto a flat plate substrate whose motion is in a circular path as shown in Figure 2. Hence, we have eliminated charging and deflection in this phase in order to systematically develop the PDM process. Cylinders are built on a flat plate substrate (instead of on a circular cylinder substrate) as a demonstration of the relative arbitrariness of the shapes that can be net-formed and to investigate issues associated with fabrication of structures with large dimensions in the direction normal to the substrate.

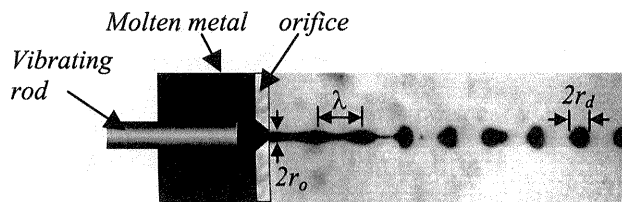


Figure 1: Photograph and sketch depicting molten droplet formation from capillary stream break-up.

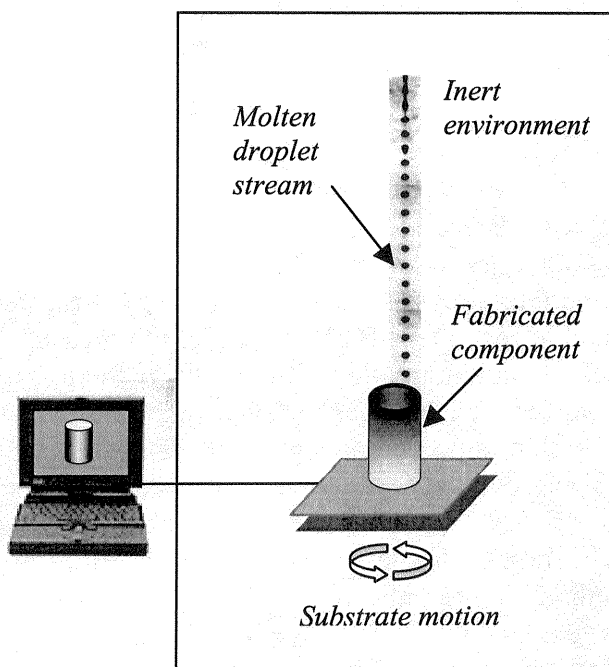


Figure 2: Conceptual schematic of cylinder fabrication on a flat-plate substrate with controlled droplet deposition.

## Experimental Considerations

As depicted in Fig. 2, the droplets are injected into an inert environment where they splat on the substrate, thereby building the net-formed component. This is necessary since the presence of oxygen in the background environment will have a deleterious effect on: 1) the basic mechanism of droplet formation from capillary streams, 2) the droplet stream stability during flight to the substrate, and 3) the quality of the fabricated component. Furthermore, the presence of aluminum oxides in the melt will also degrade the droplet stream stability, if not completely plug the orifice, since the density of the oxides are on a par with that of the aluminum alloy melt. Hence, care has been taken to filter the oxides from the melt before the jetting stage and to remove the trace oxygen elements from the background environment. The purity of the bottled gas (nitrogen or argon) is specified at 99.998%, and the oxygen level of gas in the environmental chamber is monitored to insure that the  $O_2$  level does not exceed 25 PPM. A background pressure of 14.7 psi is used in this work. More details on the apparatus are found in Reference 1.

The material used in this study was commercially available 2024 aluminum alloy. Its chemical composition was analyzed before and after filtration and jetting and was found in both cases to be consistent with industrial 2024 alloy specifications.

## Experimental Results

Uniform molten 2024 aluminum alloy droplet streams have been generated in an inert environment where they travel 50.0cm before they impinge onto the substrate. The long travel distance is not a requirement for the PDM process, but is rather imposed upon this work by means of the available apparatus. The long travel distance has not been found to degrade the stream stability (which is a significant finding in its own right), however it plays a significant role in droplet cooling during flight and droplet speed reduction due to aerodynamic drag. The latter two factors can be accounted for in model predictions.<sup>14</sup>

A photograph of a typical fabricated cylinder is shown in Figure 3. Two sections have been removed (at  $180^\circ$  separations) from the base for microstructural analysis. It is acknowledged that the component shown is preliminary, inasmuch as it does not possess the geometric smoothness required for industrial applications, yet it is included in this paper as documentation of the current state of the PDM development. Ongoing work includes the development of a numerical model for the determination of processing parameters (substrate temperature, droplet temperature, environmental temperature, and mass delivery rate to the substrate) that yield components of high geometric, mechanical, and microstructural fidelity.<sup>14</sup> Nevertheless, it is found that microstructural and mechanical analysis of components such as that shown in Figure 3 play a useful role in the development of the PDM process. Cylinders have been fabricated at heights up to 11 cm from the substrate.

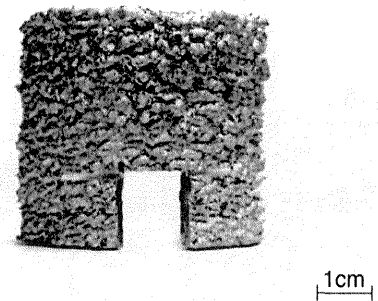


**Figure 3: Photograph of droplet deposited aluminum alloy cylinder. Two samples have been removed from the cylinder base at  $180^\circ$  separations for analysis.**

This paper reports on the microstructural results, hardness and density of six such cylinders that were fabricated over a wide range of processing parameters that are included below in Table 1. In the table,  $T_0$  is the initial capillary stream temperature,  $T_s$  is the substrate

temperature and  $m/l$  is the mass delivered per unit length to the substrate, which is directly related to the droplet speed and substrate speed. We chose not to characterize the results in terms of the mass flow rate,  $\dot{m}$ , since it contains no information regarding the amount of material overlap on the substrate (a function of substrate speed), which is of critical importance for the geometric and mechanical quality of the component. The cylinders were sectioned as indicated in Figure 3, and the sections were polished and subsequently photographed with an optical microscope. The samples were etched with a modified version of Keller's Reagent, which consists of 31%  $H_2O$ , 31%  $HCl$ , 31%  $HNO_3$  and 7%  $HF$ .

#### *Microstructural Results*

Figure 4 illustrates the microstructure of the cylindrical component shown in Figure 3. This sample has been labeled "#1" and its processing parameters are found in Table 1. It can be seen that the microstructure, which was photographed at a section 5.0 mm from the substrate surface, is on the order of  $50\mu m$ .

Figure 5 is a photomicrograph of sample #2a taken 35 mm from the substrate surface. The average grain size is also on the order of  $50\mu m$ , however, large voids can be seen in the lower center of the photograph.

Figure 6 shows the microstructure of sample #2b that was taken from the same cylinder as that of #2a, however at a distance of 6.0 mm from the substrate as opposed to 35.0 mm. Additionally, the droplet impact speed was 10 m/s in sample #2a, which was changed from 11 m/s in sample #2b. Hence,  $m/l$  was higher in sample #2b, thereby transferring more heat from the molten droplet stream to the cylinder. Therefore, there exist two reasons for greater exposure to heat in sample #2b

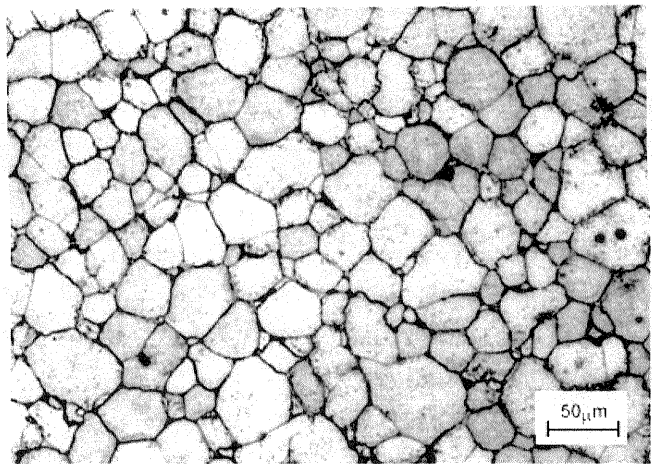


Figure 4: Microstructure of cylinder #1.

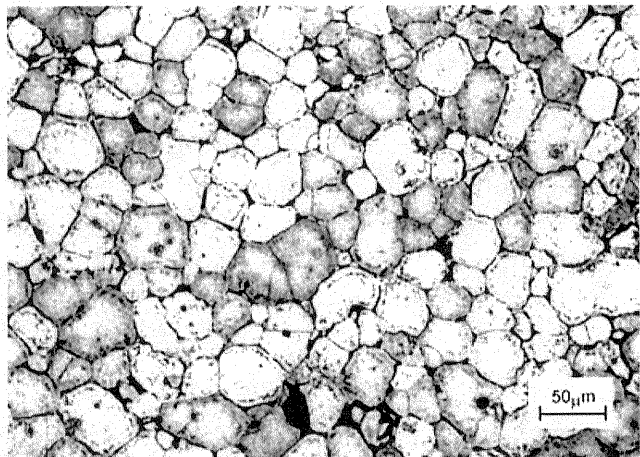


Figure 5: Microstructure of cylinder #2a.

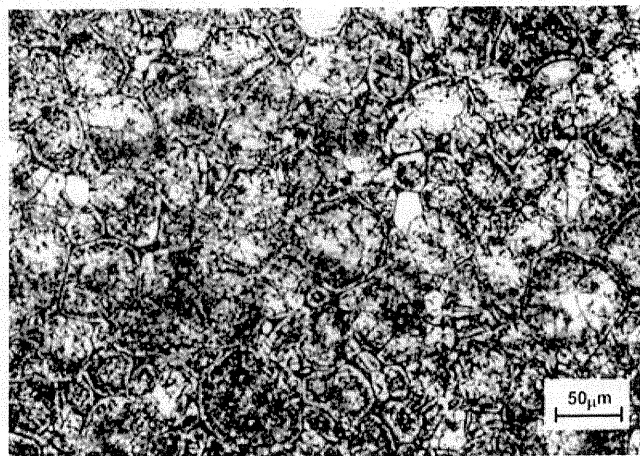


Figure 6: Microstructure of sample #2b

than in sample #2a: 1) increased heat transfer due to higher values of  $m/l$ , and 2) closer proximity to the heated substrate. This is one explanation for the coarser precipitates in the microstructure of Figure 6.

The microstructure shown in Figure 7 was taken from sample #3, at a distance of 10.0 cm from the substrate. Again, the grains are typically on the order of 50  $\mu\text{m}$ . This result is significant, since it is clear that components can be fabricated at relatively great distances from the substrate surface with little change in microstructure or hardness.

Figure 8 is a photograph of the microstructure of sample #4. It is apparent that this sample possesses the largest grains of all of the specimens studied. The reason for the larger grain structure is due to the fact that the combination of the droplet temperature and the substrate temperature is higher than in any other case studied, thereby increasing the splat solidification time, which is well known to cause larger grain sizes.

The microstructure shown in Figure 9 is from a cylinder that was fabricated with an extremely high  $m/l$  compared to the other cylinders in this study (see Table 1 for sample #5) and a moderate substrate temperature. The microstructure shown occurred at a vertical distance of 20.0mm from the substrate surface. Clearly observable in the figure are dark precipitation zones, which are a result of the elevated temperature in the deposited material due to the high mass flow rate to the substrate.

Figure 10 is a photomicrograph of cylinder #6. The microstructure is distinguished by fine grains that are 10  $\mu\text{m}$  or less. The large black areas on the upper part of the photograph are not voids but rather are the irregular outer boundary of

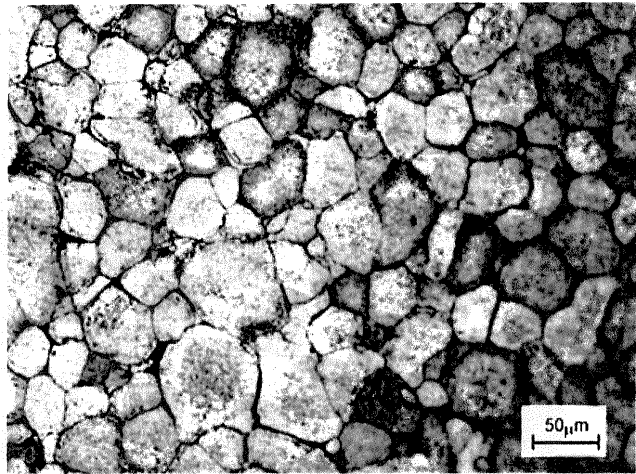


Figure 7: Microstructure of sample #3

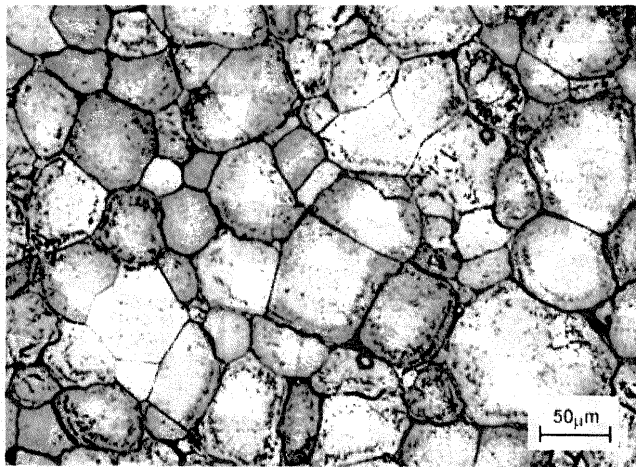


Figure 8: Microstructure of sample #4

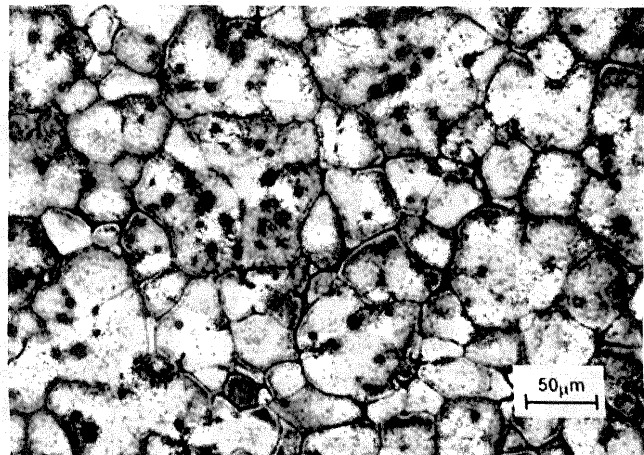


Figure 9: Microstructure of sample #5

the specimen. Unlike the other samples presented in this work, the microstructure of this sample reveals the outline of an isolated droplet that has fused relatively intact, preserving its identity. The existence of relatively refined grain structures and pristine droplet boundaries would intuitively lead to the correct judgement that the droplet and substrate temperatures were lower than in previous cases presented here. The processing parameters listed in Table 1, albeit accurate, provide misleading information for this sample, since this particular experimental realization was anomalous in the sense that the droplet stream was characterized by an angular “jitter” that greatly enhanced the convective cooling of the droplets during flight (and severely degraded the cylinder geometry). Since the droplets were no longer traveling in tandem, the aerodynamic and thermal protection of the neighboring droplet wake was eliminated, thereby causing greater droplet cooling. Hence, the droplets were much cooler than their highly stable counterparts. While the fabricated component is not useful in a practical sense, this experimental result has indicated that fine microstructures can be achieved without any loss of density as will be discussed below.

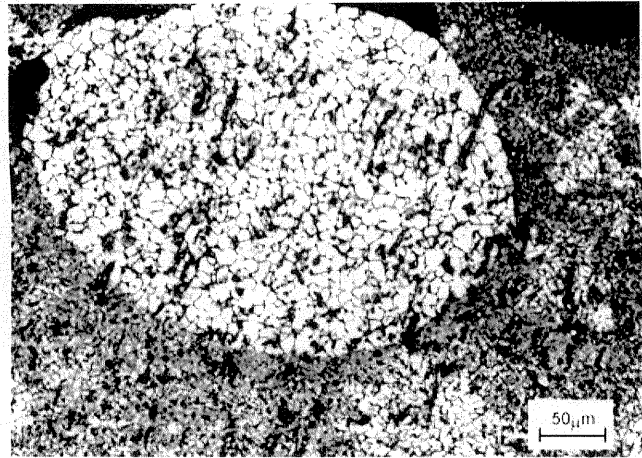


Figure 10: Microstructure of sample #6

	1	2a	2b	3	4	5	6
<b>Microstructures shown in Figure number</b>	4	5	6	7	8	9	10
<b>T<sub>o</sub> (°C)</b>	787	830	830	732	845	810	778
<b>T<sub>s</sub> (°C)</b>	176	149	149	315	454	260	460
<b>m/l (kg/m)</b>	1.02	1.04	1.19	1.65	0.82	8.53	1.10
<b>Rockwell “B” Hardness</b>	57	49	26	51	54	57	44
<b>BNH* Hardness (conversion)</b>	101	93	77	95	98	101	89
<b>Specific gravity (g/cc)</b>	2.62	2.66	2.66	2.57	2.63	2.71	2.70

Table 1: Processing parameters associated with the microstructures shown in Figures 4-10.

*Hardness*

Micro-hardness tests were conducted on each of the above samples directly after fabrication (with no post-working) at OCM Test Laboratory in Anaheim California. The results are included in Table 1 in the row entitled Rockwell “B” Hardness. The Rockwell “B” values were then converted to BNH values (500 kg load and a 10 mm diameter ball) in order to compare to the unworked 2024 reference stock which has a Rockwell “B” Hardness value of less than zero, and a BNH value of 47. Each hardness entry included in the table is the average of five readings taken over a vertical distance of 1.0 cm in the sample. The test procedure is identified as ASTM-E-384.

The samples with the greatest hardness are those that are characterized by the larger grain sizes. This finding is counter-intuitive since fine grain sizes are generally known to result in enhanced mechanical properties. However, in samples 1, 4, and 5 (which possess the highest values of hardness), the heat flux received by the cylinder during deposition (either through the delivery of large values of mass per unit length of cylinder or through high droplet temperatures) was sufficiently high to insure that the droplet material spread prior to solidification so that no pores could be embedded within the component. Hence, higher melt temperatures result in larger grain sizes, but also act to reduce porosity, thereby increasing the hardness of the component. The value of hardness for sample 2b is significantly lower than that of any of the other samples and it is concluded to be a result of the coarse precipitates which are observable in the micrographs and thought to be due to elevated heating during processing

### *Specific gravity*

The specific gravity was also measured by OCM Test Laboratories for each of the above specimens, and found to vary from 2.57 to 2.71 g/cc, where the raw stock value of 2.70 g/cc is used as a reference. Hence cylinders have been fabricated that are fully dense and devoid of measurable porosity at best and others have been fabricated with a porosity of 4.8 % at worst. A measured specific gravity greater than the reference value is believed to be due to experimental uncertainties. With the exception of the anomalous sample #6, and sample 2b with coarse precipitates, the fully dense and nearly fully dense parts are those which have the highest measured hardness. Hence, the conclusion that porosity is the cause of lower hardness is corroborated in part by these measurements. Sample #6 is peculiar inasmuch as the sample is fully dense, yet the hardness is relatively low. However, it is stressed that this sample was anomalous since the droplet stream was not stable in an angular sense, and the resulting fabricated cylinder was grossly irregular. Additionally, specimen 2b is only 1.5% less dense than our reference value, yet the hardness is significantly lower than the other samples in this work. Hence, the generation of *widespread coarse precipitates* appears to be the influencing factor for the generation of softer components and porosity is of secondary importance. Alternatively, the generation of *somewhat finer precipitates*, such as those in specimen #5 acts to harden the component.

### **Summary**

Several important findings have been reported in this paper which chronicles the development of the PDM process and are summarized here. The five most important findings are that: 1) molten aluminum alloy 2024 droplet streams can be generated from capillary stream break-up and travel a distance of 50.0 cm in an inert environment without observable degradation in stream uniformity (it is believed that this is the first time such a result has been reported); 2) it has been found that structures as high as 11.0 cm can be formed (11.0 cm is the greatest height that our current apparatus will permit) with little measurable changes in component characteristics; 3) BNH of as-deposited material is roughly twice that of (annealed) raw stock; 4) 2024 droplets can be generated and deposited without deviation from specified alloy composition limits and 5) fully dense components can be fabricated.

The processing parameters that govern the mechanical and microstructural integrity of the net-formed component are coupled with each other. It has been found that the most important factor is the heat flux received by the cylinder during droplet deposition. The heat flux can be affected by varying the mass delivered per unit length, the droplet temperature or the substrate

temperature. Extreme heating of the cylinder through any of the mechanisms discussed above results in coarsely precipitated microstructure, which can reduce the hardness of the component. Additionally, extreme heat fluxes also thickened cylinder walls due to slow solidification times. It is also important, however, that the droplets not be too cool prior to impingement, else the droplet boundaries will remain intact thereby reducing the structural integrity of the component. Hence, there is a trade-off between high heat fluxes to reduce porosity and increase hardness, and low heat fluxes for higher control over component geometry and finer microstructures.

### Acknowledgements

The authors wish to acknowledge the generous grants from the Boeing Commercial Airplane Group (grant number BCA-23483), Lawrence Livermore National Laboratories (grant number B345710), and the National Science Foundation (grant number DMI-9622400).

### References

- <sup>1</sup> Orme M., and Smith, R. "Enhanced Aluminum Properties with Precise Droplet Deposition" *ASME Journal of Manufacturing Science and Engineering*, under review, 1999
- <sup>2</sup> Sweet R. G. "High-Frequency Oscillography with Electrostatically Deflected Ink Jets," *Stanford Electronics Laboratories Technical Report No. 1722-1*, Stanford University, CA, 1964
- <sup>3</sup> Sweet R. G. "High Frequency Recording with Electrostatically Deflected Ink Jets", *Rev. Sci. Instrum.* 36, 2, 131, 1965
- <sup>4</sup> Orme M., Liu Q., and Huang, C., "Mutual Electrostatic Interactions between Closely Spaced Charged Solder Droplets, *Submitted* 1999
- <sup>5</sup> Rayleigh, Lord, [1879] On the instability of jets. *Proc. London Math. Soc.* 10, 4-13
- <sup>6</sup> Bidone, G. Experiences sur la forme et sur la direction des veines et des courants d'eau lances par diverses ouvertures. *Imp. Royale*, Turin, 1829
- <sup>7</sup> Savart, F. "Memoire sur la constitution des veines lequides lancees par des orifices circulaires en mince paroi" *Annales de Chimie et de Physique* 53, 1833
- <sup>8</sup> Orme M, "On the Genesis of Droplet Stream Microspeed Dispersions," *Physics of Fluids*, 3, (12) 1991
- <sup>9</sup> Prinz, F.B., Weiss, L.E., Amon, C.H. and Beuth, J.L., 1995, "Processing, Thermal and Mechanical Issues in Shape Deposition Manufacturing" *Solid Freeform Fabrication Symposium*, Austin, Texas, 118-129
- <sup>10</sup> Amon, C.H., Schmaltz, K.S., Merz, R., Prinz, F.B., 1996 "Numerical and Experimental Investigation of Interface Bonding Via Substrate Remelting of an Impinging Molten Metal Droplet" *ASME J. of Heat Transfer*, 118, 164-172
- <sup>11</sup> Amon, C.H., Beuth, J.L., Merz, R., Prinz, F.B., and Weiss. L.E., 1998, "Shape Deposition Manufacturing with Microcasting: Processing, Thermal and Mechanical Issues, *ASME J. Manufacturing Science and Engineering*, Vol. 120, pp 656-667
- <sup>12</sup> Chin, R.K., Beuth, J.L., and Amon, C.H., 1996 "Thermomechanical Modeling of Molten Metal Droplet Solidification Applied to Layered Manufacturing," *Mechanics of Materials*, Vol. 24, pp 257-271
- <sup>13</sup> Sachs E., Cima M., Williams P., Brancazio D., Cornie J., 1992, *J. of Eng. For Ind.*, 114, 4, 481-488
- <sup>14</sup> Shapiro, A. and Orme, Melissa, 1999, "Numerical Modeling for Droplet-Based Net-Form Manufacturing", a collaborative effort between Lawrence Livermore National Laboratory and UCI.